Longitudinal spin transfer to Λ and Λ̄ hyperons in polarized proton-proton collisions at s√=200 GeV

(STAR Collaboration) Abelev, B. I.; ...; Planinić, Mirko; ...; Poljak, Nikola; ...; Zoulkarneeva, Y.

Longitudinal spin transfer to Λ and $\bar{\Lambda}$ hyperons in polarized proton-proton collisions at $\sqrt{s} = 200\,\text{GeV}$

B. I. Abelev,[8] M. M. Aggarwal,[30] Z. Ahammed,[47] A. V. Alakhverdyants,[17] B. D. Anderson,[18] D. Arkhipkin,[3]
G. S. Averichev,[17] J. Balewski,[22] O. Barannikova,[8] L. S. Barnby,[2] S. Baumgart,[52] D. R. Beavis,[3] R. Bellwied,[50]
F. Benedosso,[27] M. J. Betancourt,[22] R. R. Betts,[8] A. Bhasin,[16] A. K. Bhati,[30] H. Bichsel,[49] J. Bielcik,[10] J. Bielcikova,[11]
B. Biritz,[6] L. C. Bland,[3] I. Bnzarov,[17] B. E. Bonner,[36] J. Bouchet,[18] E. Braidot,[27] A. V. Brandin,[25] A. Bridgeman,[1]
E. Bruna,[52] S. Bueltmann,[29] T. P. Burton,[2] X. Z. Cai,[40] H. Caines,[52] M. Calderón de la Barca Sánchez,[5] O. Catu,[52]
D. Cebra,[5] R. Cendejas,[6] M. C. Cervantes,[42] Z. Chajecki,[28] P. Chaloupka,[11] S. Chattopadhyay,[47] H. F. Chen,[38] J. H. Chen,[40]
J. Y. Chen,[51] J. Cheng,[44] M. Cherney,[9] A. Chikanian,[52] K. E. Choi,[34] W. Christie,[3] P. Chung,[11] R. F. Clarke,[42]
M. J. M. Codrington,[42] R. Corliss,[22] J. G. Cramer,[49] H. J. Crawford,[4] D. Das,[5] S. Dash,[13] L. C. De Silva,[50] R. R. Debbe,[3]
T. G. Dedovich,[17] M. DePhillips,[3] A. A. Derevschikov,[32] R. Derradi de Souza,[7] L. Didenko,[3] P. Djawotho,[42] S. M. Dogra,[16]
X. Dong,[21] J. L. Drachenberg,[42] J. E. Draper,[5] J. C. Dunlop,[3] M. R. Dutta Mazumdar,[47] L. G. Efimov,[17] E. Elhalhuli,[2]
M. Elnimr,[50] J. Engelage,[4] G. Eppley,[36] B. Erazmus,[41] M. Estienne,[41] L. Eun,[31] P. Fachini,[3] R. Fatemi,[19] J. Fedorisin,[17]
R. G. Fersch,[19] P. Filip,[17] E. Finch,[52] V. Fine,[3] Y. Fisyak,[3] C. A. Gagliardi,[42] D. R. Gangadharan,[6] M. S. Ganti,[47]
E. J. Garcia-Solis,[8] A. Geromitsos,[41] F. Geurts,[36] V. Ghazikhanian,[6] P. Ghosh,[47] Y. N. Gorbunov,[9] A. Gordon,[3]
O. Grebenyuk,[21] D. Grosnick,[46] B. Grube,[34] S. M. Guertin,[6] A. Gupta,[16] N. Gupta,[16] W. Guryn,[3] B. Haag,[5] T. J. Hallman,[3]
A. Hamed,[42] L-X. Han,[40] J. W. Harris,[52] J. P. Hays-Wehle,[22] M. Heinz,[52] S. Heppelmann,[31] A. Hirsch,[33] E. Hjort,[21]
A. M. Hoffman,[22] G. W. Hoffmann,[43] D. J. Hofman,[8] R. S. Hollis,[8] H. Z. Huang,[6] T. J. Humanic,[28] L. Huo,[42] G. Igo,[6]
A. Iordanova,[8] P. Jacobs,[21] W. W. Jacobs,[15] P. Jakl,[11] C. Jena,[13] F. Jin,[40] C. L. Jones,[22] P. G. Jones,[2] J. Joseph,[18] E. G. Judd,[4]
S. Kabana,[41] K. Kajimoto,[43] K. Kang,[44] J. Kapitan,[11] K. Kauder,[8] D. Keane,[18] A. Kechechyan,[17] D. Kettler,[49]
V. Yu. Khodyrev,[32] D. P. Kikola,[21] J. Kiryluk,[21] A. Kisiel,[48] S. R. Klein,[21] A. G. Knospe,[52] A. Kocoloski,[22] D. D. Koetke,[46]
T. Kollegger,[12] J. Konzer,[33] M. Kopytine,[18] I. Koralt,[29] W. Korsch,[19] L. Kotchenda,[25] V. Kouchpil,[11] P. Kravtsov,[25]
V. I. Kravtsov,[32] K. Krueger,[1] M. Krus,[10] L. Kumar,[30] P. Kurnadi,[6] M. A. C. Lamont,[3] J. M. Landgraf,[3] S. LaPointe,[50]
J. Lauret,[3] A. Lebedev,[3] R. Lednicky,[17] C-H. Lee,[34] J. H. Lee,[3] W. Leight,[22] M. J. LeVine,[3] C. Li,[38] N. Li,[51] X. Li,[33] Y. Li,[44]
Z. Li,[51] G. Lin,[52] S. J. Lindenbaum,[26] M. A. Lisa,[28] F. Liu,[51] H. Liu,[5] J. Liu,[36] T. Ljubicic,[3] W. J. Llope,[36] R. S. Longacre,[3]
W. A. Love,[3] Y. Lu,[38] T. Ludlam,[3] G. L. Ma,[40] Y. G. Ma,[40] D. P. Mahapatra,[13] R. Majka,[52] O. I. Mall,[5] L. K. Mangotra,[16]
R. Manweiler,[46] S. Margetis,[18] C. Markert,[43] H. Masui,[21] H. S. Matis,[21] Yu. A. Matulenko,[32] D. McDonald,[36]
T. S. McShane,[9] A. Meschanin,[32] R. Milner,[22] N. G. Minaev,[32] S. Mioduszewski,[42] A. Mischke,[27] M. K. Mitrovski,[12]
B. Mohanty,[47] D. A. Morozov,[32] M. G. Munhoz,[37] B. K. Nandi,[14] C. Nattrass,[52] T. K. Nayak,[47] J. M. Nelson,[2]
P. K. Netrakanti,[33] M. J. Ng,[4] L. V. Nogach,[32] S. B. Nurushev,[32] G. Odyniec,[21] A. Ogawa,[3] H. Okada,[3] V. Okorokov,[25]
D. Olson,[21] M. Pachr,[10] B. S. Page,[15] S. K. Pal,[47] Y. Pandit,[18] Y. Panebratsev,[17] T. Pawlak,[48] T. Peitzmann,[27]
V. Perevoztchikov,[3] C. Perkins,[4] W. Peryt,[48] S. C. Phatak,[13] P. Pile,[3] M. Planinic,[53] M. A. Ploskon,[21] J. Pluta,[48] D. Plyku,[29]
N. Poljak,[53] A. M. Poskanzer,[21] B. V. K. S. Potukuchi,[16] D. Prindle,[49] C. Pruneau,[50] N. K. Pruthi,[30] P. R. Pujahari,[14]
J. Putschke,[52] R. Raniwala,[35] S. Raniwala,[35] R. L. Ray,[43] R. Redwine,[22] R. Reed,[5] J. M. Rehberg,[12] H. G. Ritter,[21]
J. B. Roberts,[36] O. V. Rogachevskiy,[17] J. L. Romero,[5] A. Rose,[21] C. Roy,[41] L. Ruan,[3] M. J. Russcher,[27] R. Sahoo,[41]
S. Sakai,[6] I. Sakrejda,[21] T. Sakuma,[22] S. Salur,[21] J. Sandweiss,[52] J. Schambach,[43] R. P. Scharenberg,[33] N. Schmitz,[23]
T. R. Schuster,[12] J. Seele,[22] J. Seger,[9] I. Selyuzhenkov,[15] P. Seyboth,[23] E. Shahaliev,[17] M. Shao,[38] M. Sharma,[50] S. S. Shi,[51]
E. P. Sichtermann,[21] F. Simon,[23] R. N. Singaraju,[47] M. J. Skoby,[33] N. Smirnov,[52] P. Sorensen,[3] J. Sowinski,[15]
H. M. Spinka,[1] B. Srivastava,[33] T. D. S. Stanislaus,[46] D. Staszak,[6] J. R. Stevens,[15] R. Stock,[12] M. Strikhanov,[25]
B. Stringfellow,[33] A. A. P. Suaide,[37] M. C. Suarez,[8] N. L. Subba,[18] M. Sumbera,[11] X. M. Sun,[21] Y. Sun,[38] Z. Sun,[20]
B. Surrow,[22] T. J. M. Symons,[21] A. Szanto de Toledo,[37] J. Takahashi,[7] A. H. Tang,[3] Z. Tang,[38] L. H. Tarini,[50]
T. Tarnowsky,[24] D. Thein,[43] J. H. Thomas,[21] J. Tian,[40] A. R. Timmins,[50] S. Timoshenko,[25] D. Tlusty,[11] M. Tokarev,[17]
T. A. Trainor,[49] V. N. Tram,[21] S. Trentalange,[6] R. E. Tribble,[42] O. D. Tsai,[6] J. Ulery,[33] T. Ullrich,[3] D. G. Underwood,[1]
G. Van Buren,[3] G. van Nieuwenhuizen,[22] J. A. Vanfossen, Jr.,[18] R. Varma,[14] G. M. S. Vasconcelos,[7] A. N. Vasiliev,[32]
F. Videbaek,[3] Y. P. Viyogi,[47] S. Vokal,[17] S. A. Voloshin,[50] M. Wada,[43] M. Walker,[22] F. Wang,[33] G. Wang,[6] H. Wang,[24]
J. S. Wang,[20] Q. Wang,[33] X. Wang,[44] X. L. Wang,[38] Y. Wang,[44] G. Webb,[19] J. C. Webb,[46] G. D. Westfall,[24] C. Whitten, Jr.,[6]
H. Wieman,[21] S. W. Wissink,[15] R. Witt,[45] Y. Wu,[51] W. Xie,[33] N. Xu,[21] Q. H. Xu,[39] W. Xu,[6] Y. Xu,[38] Z. Xu,[3] L. Xue,[40]
Y. Yang,[20] P. Yepes,[36] K. Yip,[3] I-K. Yoo,[34] Q. Yue,[44] M. Zawisza,[48] H. Zbroszczyk,[48] W. Zhan,[20] S. Zhang,[40]
W. M. Zhang,[18] X. P. Zhang,[21] Y. Zhang,[21] Z. P. Zhang,[38] Y. Zhao,[38] C. Zhong,[40] J. Zhou,[36] W. Zhou,[39] X. Zhu,[44]
Y-H. Zhu,[40] R. Zoulkarneev,[17] and Y. Zoulkarneeva[17]

(STAR Collaboration)

[1]*Argonne National Laboratory, Argonne, Illinois 60439, USA*
[2]*University of Birmingham, Birmingham, United Kingdom*
[3]*Brookhaven National Laboratory, Upton, New York 11973, USA*
[4]*University of California, Berkeley, California 94720, USA*
[5]*University of California, Davis, California 95616, USA*
[6]*University of California, Los Angeles, California 90095, USA*
[7]*Universidade Estadual de Campinas, Sao Paulo, Brazil*
[8]*University of Illinois at Chicago, Chicago, Illinois 60607, USA*
[9]*Creighton University, Omaha, Nebraska 68178, USA*
[10]*Czech Technical University in Prague, FNSPE, Prague, 115 19, Czech Republic*
[11]*Nuclear Physics Institute AS CR, 250 68 Řež/Prague, Czech Republic*
[12]*University of Frankfurt, Frankfurt, Germany*
[13]*Institute of Physics, Bhubaneswar 751005, India*
[14]*Indian Institute of Technology, Mumbai, India*
[15]*Indiana University, Bloomington, Indiana 47408, USA*
[16]*University of Jammu, Jammu 180001, India*
[17]*Joint Institute for Nuclear Research, Dubna, 141 980, Russia*
[18]*Kent State University, Kent, Ohio 44242, USA*
[19]*University of Kentucky, Lexington, Kentucky 40506-0055, USA*
[20]*Institute of Modern Physics, Lanzhou, China*
[21]*Lawrence Berkeley National Laboratory, Berkeley, California 94720, USA*
[22]*Massachusetts Institute of Technology, Cambridge, Massachusetts 02139-4307, USA*
[23]*Max-Planck-Institut für Physik, Munich, Germany*
[24]*Michigan State University, East Lansing, Michigan 48824, USA*
[25]*Moscow Engineering Physics Institute, Moscow, Russia*
[26]*City College of New York, New York City, New York 10031, USA*
[27]*NIKHEF and Utrecht University, Amsterdam, The Netherlands*
[28]*The Ohio State University, Columbus, Ohio 43210, USA*
[29]*Old Dominion University, Norfolk, Virginia 23529, USA*
[30]*Panjab University, Chandigarh 160014, India*
[31]*Pennsylvania State University, University Park, Pennsylvania 16802, USA*
[32]*Institute of High Energy Physics, Protvino, Russia*
[33]*Purdue University, West Lafayette, Indiana 47907, USA*
[34]*Pusan National University, Pusan, Republic of Korea*
[35]*University of Rajasthan, Jaipur 302004, India*
[36]*Rice University, Houston, Texas 77251, USA*
[37]*Universidade de Sao Paulo, Sao Paulo, Brazil*
[38]*University of Science & Technology of China, Hefei 230026, China*
[39]*Shandong University, Jinan, Shandong 250100, China*
[40]*Shanghai Institute of Applied Physics, Shanghai 201800, China*
[41]*SUBATECH, Nantes, France*
[42]*Texas A&M University, College Station, Texas 77843, USA*
[43]*University of Texas, Austin, Texas 78712, USA*
[44]*Tsinghua University, Beijing 100084, China*
[45]*United States Naval Academy, Annapolis, Maryland 21402, USA*
[46]*Valparaiso University, Valparaiso, Indiana 46383, USA*
[47]*Variable Energy Cyclotron Centre, Kolkata 700064, India*
[48]*Warsaw University of Technology, Warsaw, Poland*
[49]*University of Washington, Seattle, Washington 98195, USA*
[50]*Wayne State University, Detroit, Michigan 48201, USA*
[51]*Institute of Particle Physics, CCNU (HZNU), Wuhan 430079, China*
[52]*Yale University, New Haven, Connecticut 06520, USA*
[53]*University of Zagreb, Zagreb, HR-10002, Croatia*

The longitudinal spin transfer, D_{LL}, from high energy polarized protons to Λ and $\bar{\Lambda}$ hyperons has been measured for the first time in proton-proton collisions at $\sqrt{s} = 200$ GeV with the STAR detector at the Relativistic Heavy Ion Collider. The measurements cover pseudorapidity, η, in the range $|\eta| < 1.2$ and

transverse momenta, p_T, up to 4 GeV/c. The longitudinal spin transfer is found to be $D_{LL} = -0.03 \pm$ 0.13(stat) $\pm$ 0.04(syst) for inclusive Λ and $D_{LL} = -0.12 \pm 0.08$(stat) ± 0.03(syst) for inclusive $\bar{\Lambda}$ hyperons with $\langle \eta \rangle = 0.5$ and $\langle p_T \rangle = 3.7$ GeV/c. The dependence on η and p_T is presented.

The longitudinal spin transfer to Λ and $\bar{\Lambda}$ hyperons has been studied in $e^+ e^-$ collisions at LEP [1,2] and in deep-inelastic scattering of neutrinos [3], polarized muons [4,5], and polarized positrons [6] on unpolarized targets. The phenomenon is understood to originate from different physical mechanisms in the different types of reactions. At LEP, the fragmentation of highly polarized strange quark and antiquark pairs is expected to dominate. In deep-inelastic scattering, the spin transfer from struck quarks and target fragments is expected to play an important role [7].

In this paper, we study the longitudinal spin transfer, D_{LL}, to Λ and $\bar{\Lambda}$ hyperons produced in polarized proton-proton collisions at $\sqrt{s} = 200$ GeV center-of-mass energy,

$$D_{LL} \equiv \frac{\sigma_{p^+ p \to \Lambda^+ X} - \sigma_{p^+ p \to \Lambda^- X}}{\sigma_{p^+ p \to \Lambda^+ X} + \sigma_{p^+ p \to \Lambda^- X}}, \qquad (1)$$

where the superscripts $+$ and $-$ denote helicity. The production cross section has been measured for transverse momenta, p_T, up to about 5 GeV/c and is reasonably well described by perturbative QCD evaluations for a suitable choice of fragmentation functions [8]. Within this framework, the production cross sections are described in terms of calculable partonic cross sections and nonperturbative parton distribution and fragmentation functions. The spin transfer D_{LL} is thus expected to be sensitive to polarized parton distribution functions and polarized fragmentation functions. Present data are too scarce to adequately constrain the polarized fragmentation functions. Sizable uncertainties also remain in the polarized parton distributions, particularly in the polarized sea quark and gluon distributions. This is reflected in the model predictions for D_{LL} at the Relativistic Heavy Ion Collider (RHIC) [9–13].

The polarization of Λ ($\bar{\Lambda}$) hyperons, $P_{\Lambda(\bar{\Lambda})}$, can be measured via the weak decay channel $\Lambda \to p\pi^-$ ($\bar{\Lambda} \to \bar{p}\pi^+$) from the angular distribution of the final state,

$$\frac{dN}{d\cos\theta^*} = \frac{\sigma \mathcal{L} A}{2}(1 + \alpha_{\Lambda(\bar{\Lambda})} P_{\Lambda(\bar{\Lambda})} \cos\theta^*), \qquad (2)$$

where σ is the (differential) production cross section, $\mathcal{L}$ is the integrated luminosity, A is the detector acceptance, which may vary with θ^* as well as other observables, and $\alpha_\Lambda = -\alpha_{\bar{\Lambda}} = 0.642 \pm 0.013$ [14] is the weak decay parameter. In this paper, the polarization along the Λ ($\bar{\Lambda}$) momentum direction is considered and θ^* is the angle between the polarization direction and the (anti-)proton momentum in the Λ ($\bar{\Lambda}$) rest frame. The spin transfer

D_{LL} in Eq. (1) is identical to $P_{\Lambda(\bar{\Lambda})}$ if the proton beam polarization is maximal.

The data were collected at the RHIC with the solenoidal tracker at RHIC (STAR) [15] in the year 2005. An integrated luminosity of 2 pb^{-1} was sampled with longitudinal proton beam spin configurations. The degree of proton polarization was measured for each beam and each beam fill using Coulomb-nuclear interference proton-carbon polarimeters [16], which were calibrated *in situ* using a polarized atomic hydrogen gas-jet target [17]. The average longitudinal polarizations for the two beams were 52% $\pm$ 3% and 48% $\pm$ 3% for the analyzed data. Different beam spin configurations were used for successive beam bunches and the pattern was changed between beam fills to minimize systematic uncertainties. The data were sorted by beam spin configuration.

Beam-beam counters (BBC) at both sides of the STAR interaction region were used to signal proton beam collision events, to measure the relative luminosities for the different beam spin configurations, and to determine the size of any residual transverse beam polarization components at the STAR interaction region [18]. The BBC proton collision signal defined the minimum bias (MB) trigger condition. The data presented here were recorded with the MB trigger condition and with two additional trigger conditions. A high-tower (HT) trigger condition required the BBC proton collision signal in coincidence with a transverse energy deposit $E_T > 2.6$ GeV in at least one barrel electromagnetic calorimeter (BEMC) [19] tower, covering $\Delta\eta \times \Delta\phi = 0.05 \times 0.05$ in pseudorapidity, η, and azimuthal angle, ϕ. A jet-patch (JP) trigger condition imposed the MB condition in coincidence with an energy deposit $E_T > 6.5$ GeV in at least one of six BEMC patches each covering $\Delta\eta \times \Delta\phi = 1 \times 1$. The total BEMC coverage was $0 < \eta < 1$ and $0 < \phi < 2\pi$ in 2005. Charged particle tracks in the 0.5 T magnetic field were measured with the time projection chamber (TPC) [20], covering $0 < \phi < 2\pi$ and $|\eta| \lesssim 1.3$. The measurement of specific energy loss, dE/dx, in the TPC gas provided particle identification [21].

The Λ and $\bar{\Lambda}$ candidates were identified from the topology of their dominant weak decay channels, $\Lambda \to p\pi^-$ and $\bar{\Lambda} \to \bar{p}\pi^+$, each having a branching ratio of 63.9% [14]. The procedure closely resembled the one used in the cross section measurement reported in Ref. [8]. The reconstructed event vertex was required to be along the beam axis and within 60 cm of the TPC center to ensure uniform tracking efficiency. A sample of 1.8×10^6 events satisfying the MB trigger condition was analyzed. In addition,

2.5×10^6 events were analyzed satisfying the HT trigger condition and 3.2×10^6 events satisfying the JP trigger condition. About 0.3×10^6 of these events satisfied both HT and JP trigger requirements. A search was made in each event to find (anti-)proton and pion tracks of opposite curvature. The tracks were then paired to form a Λ ($\bar{\Lambda}$) candidate and topological selections were applied to reduce background. The selections included criteria for the distance of closest approach between the paired tracks and the distance between the point of closest approach and the beam collision vertex, and demanded that the momentum sum of the track pair pointed at the collision vertex. The criteria were tuned to preserve the signal while reducing the background fraction to 10% or less.

Figure 1(a) shows the invariant mass distribution for the Λ (filled circles) and $\bar{\Lambda}$ (open circles) candidates reconstructed from MB data with $|\eta| < 1.2$ and $0.3 < p_T < 3$ GeV/c. The mean values of the Λ and $\bar{\Lambda}$ mass distributions are in agreement with the PDG mass value $m_{\Lambda(\bar{\Lambda})} = 1.11568$ GeV/c^2 [14]. Figure 1(b) shows the same invariant mass distribution versus $\cos\theta^*$ for the Λ candidates. The number of Λ candidates varies with $\cos\theta^*$ because of detector acceptance. The small variation of the reconstructed invariant mass with $\cos\theta^*$ is understood to originate from detector resolution. In addition to signal and combinatorial background, backgrounds are seen of misidentified e^+e^- pairs at low invariant mass values near $\cos\theta^* = -1.0$ and of misidentified K_S^0 in a diagonal band at high invariant mass values and $\cos\theta^* > -0.2$. About 1.2×10^4 Λ and 1.0×10^4 $\bar{\Lambda}$ candidates with reconstructed invariant mass $1.109 < m < 1.121$ GeV/c^2 were kept for further analysis. The average residual background fraction was determined to be about 9% by averaging the candidate counts in the mass intervals $1.094 < m < 1.103$ GeV/c^2 and $1.127 < m < 1.136$ GeV/c^2.

The observed spectra are affected by detector resolution and acceptance. To minimize the uncertainty associated with acceptance effects, D_{LL} has been extracted in small
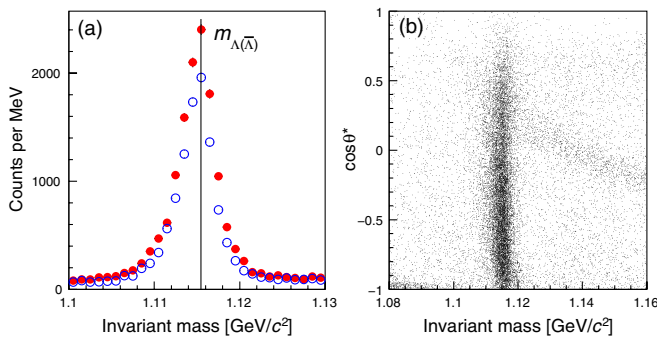

FIG. 1 (color online). (a) The invariant mass distribution of Λ (filled circles) and $\bar{\Lambda}$ (open circles) candidates from reconstructed $p + \pi^-$ and $\bar{p} + \pi^+$ track pairs in 2005 MB data after topological selections. (b) The invariant mass distribution versus $\cos\theta^*$ for Λ.

intervals in $\cos\theta^*$ from the ratio:

$$D_{LL} = \frac{1}{\alpha P_{\text{beam}} \langle \cos\theta^* \rangle} \frac{N^+ - RN^-}{N^+ + RN^-}, \qquad (3)$$

where α is the decay parameter, P_{beam} is the measured polarization for either RHIC beam, and $\langle \cos\theta^* \rangle$ denotes the average in the $\cos\theta^*$ interval. Equation (3) follows from Eqs. (1) and (2), and parity conservation in the hyperon production processes considered here. The single spin hyperon yield N^+ was obtained by summing the double spin yields n^{++} and n^{+-} weighted by the relative luminosity for the $++$ and $+-$ beam spin configurations. The yield N^- was obtained in a similar way from n^{-+} and n^{--}, and R denotes the relative luminosity ratio to normalize N^+ and N^-. The single spin yield N^+ can also be determined from the alternative combination of double spin yields, n^{++} and n^{-+}, as if the other beam is (un-)polarized. In this case N^- is obtained from n^{+-} and n^{--}.

The yields N^+ and N^- were determined for each $\cos\theta^*$ interval from the observed Λ and $\bar{\Lambda}$ candidate yields in the mass interval from 1.109 to 1.121 GeV/c^2. The corresponding raw values D_{LL}^{raw} were averaged over the entire $\cos\theta^*$ range. The obtained D_{LL}^{raw} values and their statistical uncertainties were then corrected for (unpolarized) background dilution according to $D_{LL} = D_{LL}^{\text{raw}}/(1 - r)$, where r is the average background fraction. No significant spin transfer asymmetry was observed for the yields in the sideband mass intervals $1.094 < m < 1.103$ GeV/c^2 and $1.127 < m < 1.136$ GeV/c^2, and thus no further correction was applied to D_{LL}. However, a contribution was included in the estimated systematic uncertainty of the D_{LL} measurement to account for the possibility that the background could nevertheless be polarized. Its size was determined by the precision of the spin transfer asymmetries for the sideband mass intervals. The D_{LL} results obtained with either of the beams polarized were combined, taking into account the overlap in the event samples.

Figure 2(a) shows the combined D_{LL} results from the MB data sample versus $\cos\theta^*$ for the inclusive production of Λ hyperons with $0.3 < p_T < 3$ GeV/c and $0 < \eta < 1.2$ and $-1.2 < \eta < 0$. The results for the $\bar{\Lambda}$ hyperon are shown in Fig. 2(b). Positive η is defined along the direction of the incident polarized beam. Fewer than 50 counts were observed for $\cos\theta^* > 0.9$ and this interval was discarded for this reason. The extracted D_{LL} is constant with $\cos\theta^*$, as expected and confirmed by the quality of fit. In addition, a null measurement was performed of the spin transfer for the spinless K_S^0 meson, which has a similar event topology. The K_S^0 candidate yields for $|\cos\theta^*| > 0.8$ were discarded since they have sizable Λ ($\bar{\Lambda}$) backgrounds. The result, δ_{LL}, obtained with an artificial weak decay parameter $\alpha_{K_S^0} = 1$, was found consistent with no spin transfer, as shown in Fig. 2(c). The analysis was furthermore tested with simulated Λ data having a nonzero D_{LL} and the D_{LL} input to the simulation was extracted successfully.
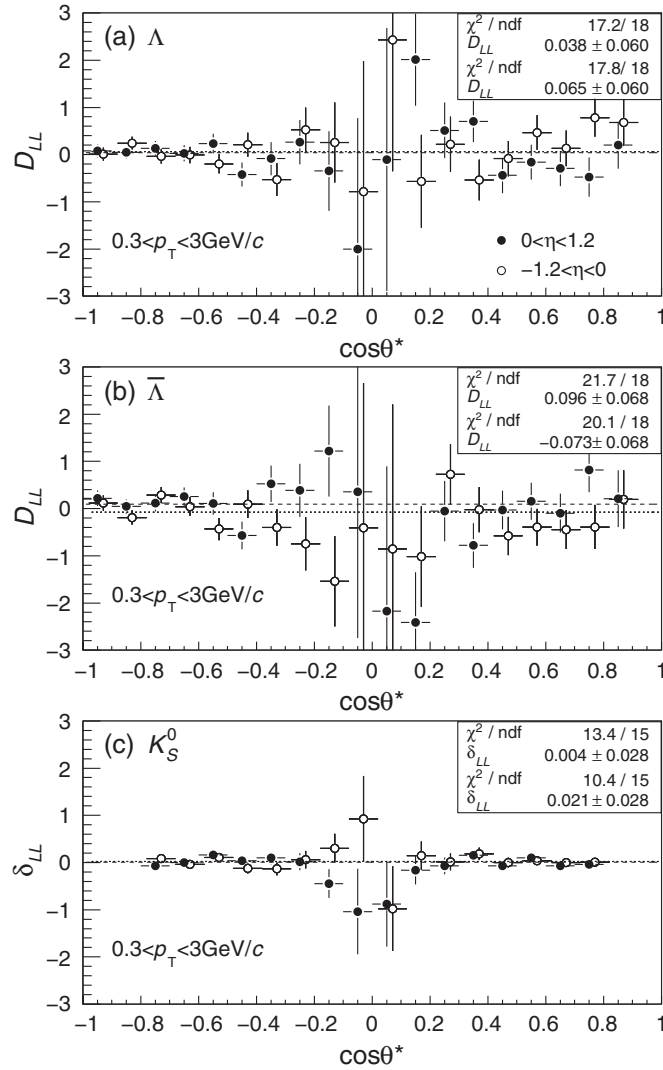
FIG. 2. The spin transfer D_{LL} versus $\cos\theta^*$ for (a) Λ and (b) $\bar{\Lambda}$ hyperons, and (c) the spin asymmetry δ_{LL} for the control sample of K_S^0 mesons versus $\cos\theta^*$. The filled circles show the results for positive pseudorapidities η with respect to the polarized beam and the open circles show the results for negative η. Only statistical uncertainties are shown. The data points with negative η have been shifted slightly in $\cos\theta^*$ for clarity. The indicated values of χ^2 and the spin transfer are for the data with positive and negative η, respectively.

In addition to the MB data, HT and JP data were analyzed. These data were recorded with trigger conditions that required large energy deposits in the BEMC and thus preferentially selected events with a hard collision. The trigger conditions did not require a highly energetic Λ or $\bar{\Lambda}$. The HT and JP data samples may thus be biased. To minimize the effects of trigger bias, the HT event sample was restricted to Λ or $\bar{\Lambda}$ candidates whose decay (anti-)proton track intersected a BEMC tower that fulfilled the trigger condition. About 50% of the $\bar{\Lambda}$ and only 3% of the Λ candidate events in the analysis pass this selection. This is qualitatively consistent with the annihilation of

antiprotons in the BEMC. The $\bar{\Lambda}$ sample that was selected in this way thus directly triggered the experiment readout. It contains about 1.0×10^4 $\bar{\Lambda}$ candidates with $1 < p_T < 5$ GeV/c and a residual background of about 5%.

In the case of the JP triggered sample, events were selected with at least one reconstructed jet that pointed to a triggered jet patch. The same jet reconstruction was used as in Refs. [22,23]. Jets outside the BEMC acceptance were rejected. The Λ and $\bar{\Lambda}$ candidates whose reconstructed η and ϕ fell within the jet cone of radius $r_{\rm cone} = \sqrt{(\Delta\eta)^2 + (\Delta\phi)^2} = 0.4$ were retained for further analysis. In most cases, the decay (anti-)proton track is part of the reconstructed jet, whereas the decay pion track is not. No correction was made to the jet finding and reconstruction for this effect. About $1.3 \times 10^4 \Lambda$ and $2.1 \times 10^4 \bar{\Lambda}$ candidates with $1 < p_T < 5$ GeV/c remain after selections. The residual background is estimated to be 13% for Λ and 9% for $\bar{\Lambda}$ candidates.

The D_{LL} analyses of the HT and JP samples are identical to that of the MB sample, and the resulting D_{LL} averaged over $\cos\theta^*$ have similar fit quality. The analysis of the corresponding K_S^0 samples shows no evidence for unaccounted systematics. The comparison of D_{LL} from MB, HT, and JP data versus p_T for positive η is shown in Fig. 3.
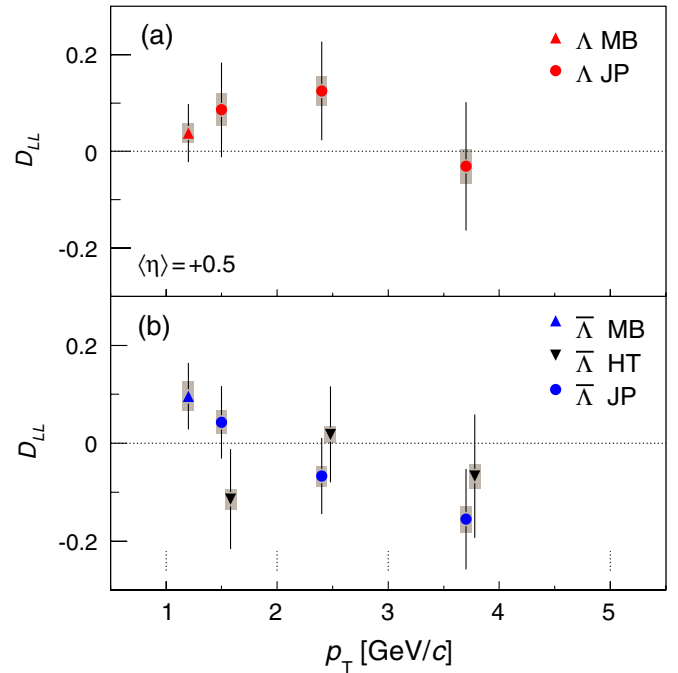

FIG. 3 (color online). The spin transfer D_{LL} to (a) Λ and (b) $\bar{\Lambda}$ hyperons produced at positive pseudorapidity with respect to the polarized proton beam from MB, JP, and HT data versus hyperon transverse momenta p_T. The sizes of the statistical and systematic uncertainties are indicated by the vertical bars and bands, respectively. For clarity, the HT data points have been shifted slightly in p_T. The dotted vertical lines indicate the p_T intervals in the analysis of HT and JP data.

Feynman x is on average about 0.02 in the interval at highest p_T.

The contributions from the uncertainties in decay parameter α and in the measurements of the proton beam polarization and relative luminosity ratios, as well as uncertainty caused by the aforementioned backgrounds, overlapping events (pileup), and, in the case of the JP sample, trigger bias, were combined in quadrature to estimate the size of the total systematic uncertainties. The effect of Λ and $\bar{\Lambda}$ spin precession in the STAR magnetic field is negligible. The above contributions are considered to be independent and their sizes have been estimated as described below.

The uncertainty in $\alpha_\Lambda = 0.642 \pm 0.013$ [14] corresponds to a 2% scale uncertainty in D_{LL}. Uncertainty in the RHIC beam polarization measurements and in the polarization angles at the STAR interaction region contribute an additional 6% scale uncertainty in D_{LL}. Uncertainties in the measurement of R are estimated to offset D_{LL} at the level of 0.01. Each of these uncertainties is common to the data from all trigger conditions. The residual backgrounds in the candidate yields differ for different trigger conditions. As described before, D_{LL} and its statistical uncertainty were corrected for unpolarized dilution and a systematic uncertainty was assigned based on the possible size of residual polarized background. This contribution to the systematic uncertainty in D_{LL} ranges from 0.01 for the MB sample to 0.03 for highest p_T in the triggered sample. The TPC data for each collision event may contain track information from multiple RHIC beam crossings. This pileup was studied by examining the observed signal candidate yields for different instantaneous beam luminosities and by extrapolating these yields to vanishingly small collision rates, for which pileup is negligible. In this way, a possible dilution of 23% in D_{LL} was estimated for MB triggered data. This was 5% for the JP data and a negligible dilution was found for the HT triggered data. The JP trigger condition biases the recorded Λ and $\bar{\Lambda}$ samples. Such effects were studied by Monte Carlo simulation of events generated with PYTHIA 6.4 [24] and the STAR detector response package based on GEANT 3 [25]. To within the $\approx 5\%$ statistical uncertainty of the simulation, no evidence was found that the JP trigger biases the gg, qg, and qq scattering contributions to the yields, or that the JP trigger biases quark over gluon fragmentation. A statistically significant reduction of about 25% in fragmentation z was observed in the simulated data when the JP trigger condition is imposed. The corresponding bias in D_{LL} is estimated to be no larger than 0.01 using D_{LL} expectations from a range of models. The simulated z value increases with increasing p_T and $z \approx 0.5$ for the data at highest p_T. The total systematic uncertainty in D_{LL} is found to increase from 0.02 to 0.04 with increasing p_T and is smaller than the statistical uncertainty, ranging from 0.06 to 0.14, for each of the data points.
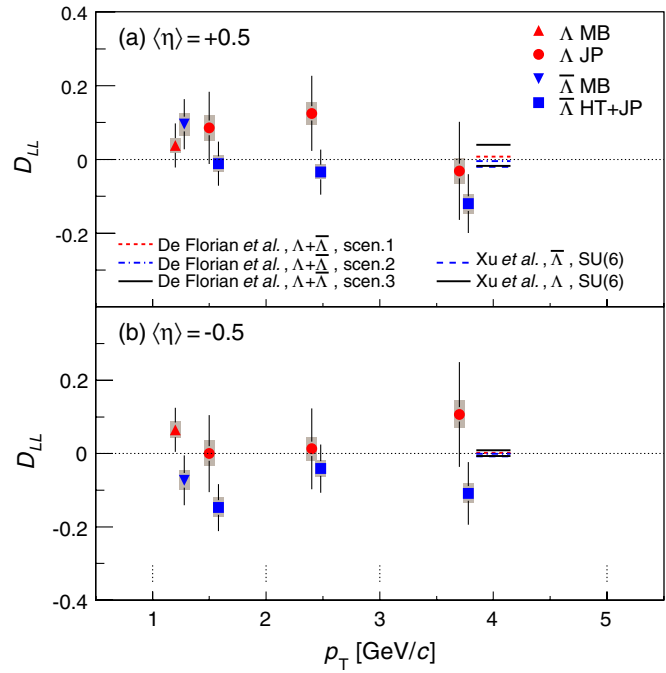

FIG. 4 (color online). Comparison of Λ and $\bar{\Lambda}$ spin transfer D_{LL} in polarized proton-proton collisions at $\sqrt{s} = 200$ GeV for (a) positive and (b) negative η versus p_T. The vertical bars and bands indicate the sizes of the statistical and systematic uncertainties, respectively. The $\bar{\Lambda}$ data points have been shifted slightly in p_T for clarity. The dotted vertical lines indicate the p_T intervals in the analysis of HT and JP data. The horizontal lines show model predictions evaluated at η and largest p_T of the data.

Figure 4 compares Λ and $\bar{\Lambda}$ D_{LL} versus p_T for positive and negative η. The $\bar{\Lambda}$ results from HT and JP data have been combined. No corrections have been applied for possible decay contributions from heavier baryonic states. The sizes of the statistical and systematic uncertainties are shown as vertical bars and shaded bands, respectively. The Λ and $\bar{\Lambda}$ results for D_{LL} are consistent with each other and consistent with no spin transfer from the polarized proton beam to the produced Λ and $\bar{\Lambda}$ to within the present uncertainties. The data have p_T up to 4 GeV/c, where $D_{LL} = -0.03 \pm 0.13\text{(stat)} \pm 0.04\text{(syst)}$ for the Λ and $D_{LL} = -0.12 \pm 0.08\text{(stat)} \pm 0.03\text{(syst)}$ for the $\bar{\Lambda}$ at $\langle\eta\rangle = 0.5$. For reference, the model predictions of Refs. [9,12,13], evaluated at $\eta = \pm 0.5$ and $p_T = 4$ GeV/c, are shown as horizontal lines. The expectations of Ref. [9] hold for Λ and $\bar{\Lambda}$ combined and examine different polarized fragmentation scenarios, in which the strange (anti-)quark carries all or only part of the Λ ($\bar{\Lambda}$) spin. The model in Refs. [12,13] separates Λ from $\bar{\Lambda}$ and otherwise distinguishes the direct production of the Λ and $\bar{\Lambda}$ from the (anti-)quark in the hard scattering and the indirect production via decay of heavier (anti-)hyperons. Both sets of expectations assume that the contribution from intrinsic gluon polarization can be neglected. The evalu-

ations are consistent with the present data and span a range of values that, for positive η, is similar to the experimental uncertainties. The measurements for negative η are less sensitive. STAR has collected additional data samples with longitudinally polarized protons in the years 2006 and 2009, and future results may be anticipated to distinguish between several of these models.

In summary, we have determined the longitudinal spin transfer to Λ and $\bar{\Lambda}$ hyperons in $\sqrt{s} = 200$ GeV polarized proton-proton collisions for hyperon p_T up to 4 GeV/c, where earlier cross section measurements are adequately described by pQCD evaluation, and have studied the η dependence. The spin transfer is found to be $D_{LL} = -0.03 \pm 0.13(\text{stat}) \pm 0.04(\text{syst})$ for Λ and $D_{LL} = -0.12 \pm 0.08(\text{stat}) \pm 0.03(\text{syst})$ for $\bar{\Lambda}$ hyperons with $\langle \eta \rangle = 0.5$ and $\langle p_T \rangle = 3.7$ GeV/c. The longitudinal spin transfer is sensitive to the polarized parton distribution and polarized fragmentation functions. The data correspond to an integrated luminosity of 2 pb^{-1} with $\approx 50\%$ beam polarization and are limited by statistics. The present results for Λ and $\bar{\Lambda}$ do not provide conclusive evidence for a spin transfer signal and have uncertainties that are comparable to the variation between model expectations for the longitudinal spin transfer at the RHIC.

[1] D. Buskulic *et al.* (ALEPH Collaboration), Phys. Lett. B **374**, 319 (1996).

[2] K. Ackerstaff *et al.* (OPAL Collaboration), Eur. Phys. J. C **2**, 49 (1998).

[3] P. Astier *et al.* (NOMAD Collaboration), Nucl. Phys. **B588**, 3 (2000); **B605**, 3 (2001).

[4] M. R. Adams *et al.* (E665 Collaboration), Eur. Phys. J. C **17**, 263 (2000).

[5] M. Alekseev *et al.* (COMPASS Collaboration), Eur. Phys. J. C **64**, 171 (2009).

[6] A. Airapetian *et al.* (HERMES Collaboration), Phys. Rev. D **64**, 112005 (2001); **74**, 072004 (2006).

[7] See e.g. C. Boros and Z. T. Liang, Phys. Rev. D **57**, 4491 (1998); J. R. Ellis, D. Kharzeev, and A. Kotzinian, Z. Phys. C **69**, 467 (1996).

[8] B. I. Abelev *et al.* (STAR Collaboration), Phys. Rev. C **75**, 064901 (2007).

[9] D. de Florian, M. Stratmann, and W. Vogelsang, Phys. Rev. Lett. **81**, 530 (1998); W. Vogelsang (private communication).

[10] C. Boros, J. T. Londergan, and A. W. Thomas, Phys. Rev. D **62**, 014021 (2000).

[11] B. Q. Ma, I. Schmidt, J. Soffer, and J. J. Yang, Nucl. Phys. **A703**, 346 (2002).

[12] Q. H. Xu, C. X. Liu, and Z. T. Liang, Phys. Rev. D **65**, 114008 (2002).

[13] Q. H. Xu, Z. T. Liang, and E. Sichtermann, Phys. Rev. D **73**, 077503 (2006); Y. Chen *et al.*, *ibid.* **78**, 054007 (2008).

[14] C. Amsler *et al.* (Particle Data Group), Phys. Lett. B **667**, 1 (2008).

[15] K. H. Ackermann *et al.* (STAR Collaboration), Nucl. Instrum. Methods Phys. Res., Sect. A **499**, 624 (2003).

[16] O. Jinnouchi *et al.*, arXiv:nucl-ex/0412053.

[17] H. Okada *et al.*, arXiv:hep-ex/0601001.

[18] J. Kiryluk (STAR Collaboration), arXiv:hep-ex/0501072.

[19] M. Beddo *et al.*, Nucl. Instrum. Methods Phys. Res., Sect. A **499**, 725 (2003).

[20] M. Anderson *et al.*, Nucl. Instrum. Methods Phys. Res., Sect. A **499**, 659 (2003).

[21] M. Shao *et al.*, Nucl. Instrum. Methods Phys. Res., Sect. A **558**, 419 (2006).

[22] B. I. Abelev *et al.* (STAR Collaboration), Phys. Rev. Lett. **97**, 252001 (2006).

[23] B. I. Abelev *et al.* (STAR Collaboration), Phys. Rev. Lett. **100**, 232003 (2008).

[24] T. Sjöstrand, S. Mrenna, and P. Skands, J. High Energy Phys. 05 (2006) 026.

[25] GEANT 3.21, CERN Program Library.